arXiv:1407.0565v1 [hep-ph] 2 Jul 2014

Remarkable Features of Decaying Hagedorn States

M Beitel, K Gallmeister and C Greiner

Institut für Theoretische Physik, Goethe-Universität Frankfurt am Main,
Max-von-Laue-Str. 1, 60438 Frankfurt am Main, Germany

E-mail: beitel@th.physik.uni-frankfurt.de

Abstract. Hagedorn states (HS) are a tool to model the hadronization process which occurs in the phase transition phase between the quark gluon plasma (QGP) and the hadron resonance gas (HRG). Their abundance is believed to appear near the Hagedorn temperature T_H which in our understanding equals the critical temperature T_c. These hadron-like resonances are characterized by being very massive and by not being limited to quantum numbers of known hadrons. To generate a whole zoo of such new states we solve the covariantly formulated bootstrap equation by regarding energy conservation and conservation of the baryon number B, strangeness S and electric charge Q. To investigate their decay properties decay chain calculations of HS were conducted. One single (heavy) HS with certain quantum numbers decays by various two-body decay channels subsequently into final stable hadrons. Multiplicities of these stable hadrons, their ratios and their energy distributions are presented. Strikingly the final energy spectra of resulting hadrons show a thermal-like distribution with the characteristic Hagedorn temperature T_H. All hadronic properties like masses, spectral functions etc. are taken from the hadronic transport model Ultra Relativistic Quantum Molecular Dynamics (UrQMD).

1. Introduciton

Before the emergence of quantum chromodynamics (QCD) as the theory of strong interactions many phenomenological ideas came up trying to describe particle production in elementary but also in heavy ion collisions. The most important idea for this note goes back to R. Hagedorn [1] who proposed in 1965 that all particles found at that time and which would be found in the future belong to a common mass spectrum. This spectrum, better known as Hagedorn spectrum, exhibits the specific feature of being exponential in the infinite mass limit. The slope of Hagedorn spectrum's exponential part is solely determined by the Hagedorn temperature T_H. This temperature denotes the limiting temperature for hadronic matter since any partition function of a HRG with Hagedorn-like mass spectrum diverges as long as $T > T_H$. Above the Hagedorn temperature a new state of matter, namely the QGP, is assumed to be realized. How a phase transition from HRG to QGP and back exactly works is one of the most challenging problems of modern physics. One possible tool to investigate this phase transition is the application of HS which mainly contribute to the exponential part of the Hagedorn spectrum but also may appear in the 'hadronic' mass range too. The HS are created in multi-particle collisions most abundantly near T_H which in our understanding equals to the critical temperature T_c. Hagedorn states are color neutral objects which are allowed to have any quantum numbers as long as they are compatible to HS' mass. The appearance of HS in multi-particle collisions and their role was already discussed in [2, 3, 4, 5, 6]. In [7, 8, 9, 10, 11, 12]. the authors show that HS can also alter the occurrence of various phases from hadronic to deconfined partonic

matter (first order, second order or crossover) improving QCD's equation of state as shown in [13, 14, 15]. The appearance of HS near T_c can explain, as shown in [4, 5, 6], the fast chemical equilibration of (multi-) strange baryons B and their anti-particles $\bar{B}$ at Relativistic Heavy Ion Collider (RHIC) energies considering HS as a kind of catalyst according to

$$\left(n_1\pi + n_2 K + n_3\overline{K} \leftrightarrow\right) HS \leftrightarrow \overline{B} + B + X. \tag{1}$$

The dynamical evolution of this reaction is given through a set of coupled rate equations leading to a chemical equilibration time of about $t_{ch} \approx 5\,\mathrm{fm}/c$ for $B\bar{B}$-pairs. Without 'clustering' of pions and kaons to HS the same approach would result at least in $t_{ch} \approx 10\,\mathrm{fm}/c$ or more which is obviously too long. The inclusion of HS in a hadron resonance gas model provides also a lowering of the speed of sound, c_s and of the shear viscosity over entropy density ratio η/s at the phase transition and being in good agreement with lattice calculations [13, 14, 16, 17]. In addition, by comparing calculations with inclusion of HS to calculations without them, a significant lowering of the shear viscosity to entropy ratio, η/s, is observed [13, 18, 19, 16]. The inclusion of HS creates a minor dependence of the thermal fit parameters of particle ratios on the Hagedorn temperature, T_H, which is assumed to be equal to T_C [20]. The successful application of HS mentioned above calls to an implementation of them into the hadronic transport program UrQMD on the basis of $2 \leftrightarrow 1$-processes by regarding the principle of detailed balance. The role of HS on dynamical evolution of multiplicities, transport coefficients etc. will thus be investigated in future [21].

2. Model

The formulation of a whole zoo of HS will be provided as they will be created in binary collisions within the microscopic hadronic transport simulation program UrQMD [22]. Multiplicities (and their ratios) of stable hadrons stemming from cascading decay simulations of one single initial massive HS for different masses, radii and quantum number combinations are calculated. Additionally energy distribution of the decay products are examined and it is shown that all hadrons stemming from that cascade follow the Boltzmann distribution analogous alike a thermalized hadron resonance gas, although the final and freely moving hadrons are freed solely from the subsequent decay. The starting point of all calculations provided is the postulate of the statistical bootstrap model (SBM) stating that fireballs consist of fireballs which in turn consist of fireballs etc. . The mathematical formulation of this postulate leads to the well known bootstrap equation

$$\begin{aligned}\tau_{\vec{C}}(m) = \frac{R^3}{3\pi m} \sum_{\vec{C}_1,\vec{C}_2} \iint \mathrm{d}m_1 \mathrm{d}m_2\, \tau_{\vec{C}_1}(m_1)\, m_1 \tau_{\vec{C}_2}(m_2)\, m_2 \\ \times\, p_{cm}(m, m_1, m_2)\, \delta_{\vec{C},\vec{C}_1+\vec{C}_2}\end{aligned} \tag{2}$$

The functions $\tau_{\vec{C}_i}$ on the r.h.s. are spectral functions of two constituents which make up a HS with spectral function τ on the l.h.s. of Eq. (2). Strict conservation of total energy leads p_{cm} denoting the momenta of both constituent particles with masses m_1 and m_2 in the rest frame of made up HS with mass m,

$$p_{cm}(m, m_1, m_2) = \frac{1}{2m}\sqrt{\left(m^2 - m_1^2 - m_2^2\right)^2 - 4m_1^2 m_2^2}, \tag{3}$$

as usual where charge conservation is assured by Kronecker's δ. The radius R denotes the size of created HS and is considered to be constant taking on some reasonable values which are discussed further below. Contrary to the well-known non-covariant bootstrap equation [23, 24],

the expression here is formulated covariantly. In the general solution of Eq. (2), the number of constituents is theoretically infinite. The reason to consider two constituents case only is because HS will be implemented in hadron transport models like e.g. UrQMD as a whole zoo of new particles. In standard transport models maximally two particles in the incoming channel are allowed because the interaction probability is calculated on the basis of geometrical cross sections. On the other hand resonance decays in two hadrons are realized in UrQMD too making an implementation of further $(2 \leftrightarrow 1)$ processes, now involving HS, possible. For this kind of new processes the principle of detailed balance will strictly hold. The accepted error by the approximation of only two outgoing particles is roughly about 30%, which can be estimated by looking at the HS decay probability into n particles, $P(n) = (\ln 2)^{n-1} / (n-1)!$, yielding a probability for the decay into two particles of 69%, into three particles of 24% etc. [23]. Given the function $\tau(m)$ we proceed to the formulation of HS' total decay width,

$$\Gamma_{\vec{C}}(m) = \frac{\sigma}{2\pi^2 \tau_{\vec{C}}(m)} \sum_{\vec{C}_1, \vec{C}_2} \iint \mathrm{d}m_1 \mathrm{d}m_2 \tau_{\vec{C}_1}(m_1) \tau_{\vec{C}_2}(m_2) \times p_{cm}^2(m, m_1, m_2) \delta_{\vec{C}, \vec{C}_1 + \vec{C}_2} \,. \tag{4}$$

This formula was derived by employing general formulae for cross section and decay width as given in [25] where for the (creation or fusion) cross section σ of HS only the $2 \to 1$ and for their decay width Γ only the $1 \to 2$ case were considered. Further we demanded the principle of detailed balance between creation and decay of HS to be valid which connects its creation with its decay properties in Eq. (4). The cross section will be considered simply as the geometrical value $\sigma = \pi R^2$. The partial decay width of a HS with mass m and charge vector $\vec{C}$ decaying into two particles with masses between m_1 and $\mathrm{d}m_1 + m_1$, m_2 and $\mathrm{d}m_2 + m_2$ and charges $\vec{C}_1$, $\vec{C}_2$ reads

$$\Delta\Gamma_{\vec{C}, \vec{C}_1, \vec{C}_2}(m, m_1, m_2) = \frac{\sigma}{2\pi^2} \frac{\Delta m_1 \tau_{\vec{C}_1}(m_1) \, \Delta m_2 \tau_{\vec{C}_2}(m_2)}{\tau_{\vec{C}}(m)} p_{cm}^2(m, m_1, m_2) \tag{5}$$

The fractional two-body branching ratios $\mathcal{B}$ are just the ratio of partial and total decay widths, Eqs. (5) and (4),

$$\Delta\mathcal{B}_{\vec{C}, \vec{C}_1, \vec{C}_2}(m, m_1, m_2) = \frac{\Delta\Gamma_{\vec{C}, \vec{C}_1, \vec{C}_2}(m, m_1, m_2)}{\Gamma_{\vec{C}}(m)} \,, \tag{6}$$

3. Results

The bootstrap equation Eq. (2) in general is a highly non-linear integral equation of Volterra type which can be solved analytically for some special cases [26, 27]. The numerical solution of the given bootstrap equation for a meson-like, non-strange and electrically neutral (B=S=Q=0) Hagedorn spectrum for two different typical radii ($R_1 = 0.8\,\mathrm{fm}, R_2 = 1.0\,\mathrm{fm}$) is presented in Fig. 1. In the same figure also spectra for baryonic non-strange and electrically charged states ($B = 1, S = 0, Q = 1$) are shown. All Hagedorn spectra rise exponentially for masses $\geq 1.5\,\mathrm{GeV}$ with different slopes for different radii, but for $m < 1.5\,\mathrm{GeV}$ they all include and thus fit the 'hadronic' part of the spectrum. The slopes of the exponential part were determined by the fit function $\tau_{\mathrm{fit}}(m) = A m^{-b} \exp(m/T_H)$, yielding the Hagedorn temperatures $T_H = 0.145\,\mathrm{GeV}$ for $R = 1.0\,\mathrm{fm}$ and $T_H = 0.162\,\mathrm{GeV}$ for $R = 0.8\,\mathrm{fm}$ both being rather independent on the chosen quantum number combinations. The total decay width of a Hagedorn state consists of three different contributions, where the first one considers only hadrons, the second hadrons and Hagedorn states, and the third one only HS in the outgoing channel as depicted in Fig. 2. The peak in the mass range of $M_{HS} = 0$-$2\,\mathrm{GeV}$ on left part of Fig. 1 comes mainly from

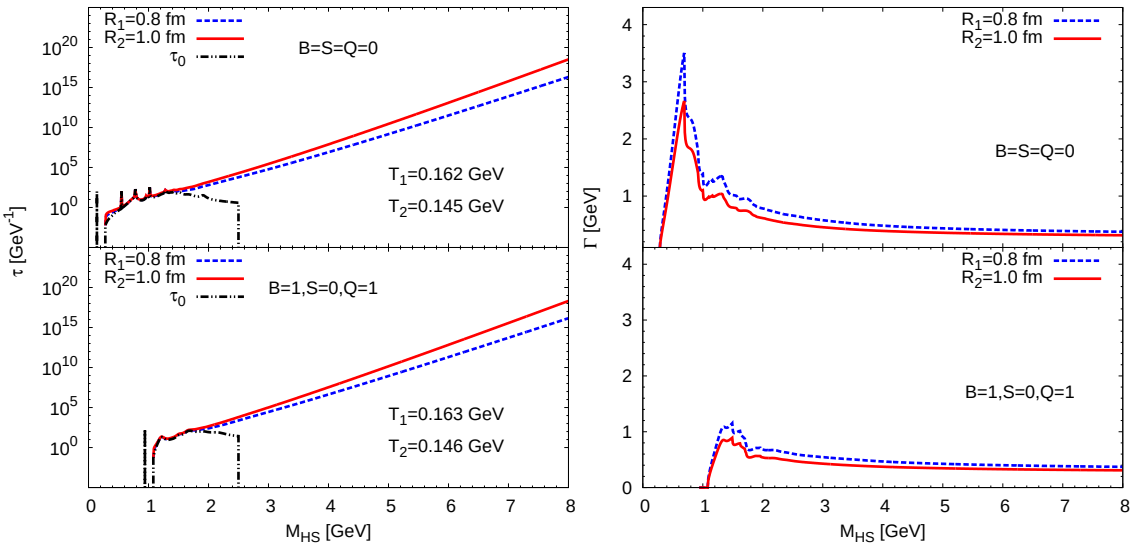

Figure 1. Meson-like ($B = S = Q = 0$) Hagedorn spectrum (upper left) and corresponding HS' total decay width (upper right) and baryonic ($B = 1, S = 0, Q = 1$) Hagedorn spectrum (lower left) and corresponding HS' total decay width (lower right) for two different radii. On the left figure additionally (fitted) Hagedorn temperatures are provided where the black line represents the sum of spectral functions of hadrons with the given quantum numbers.

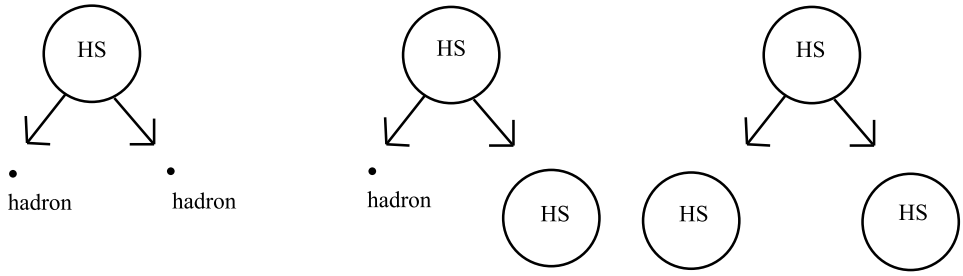

Figure 2. Decay of HS into two hadrons (left), decay into one hadron and one HS (center) and decay into two HS (right)

the first contribution, because in this mass range the phase space for pure hadronic decay is largest. The height of the peak depends on the number of hadronic pairs, whose quantum numbers all sum up to the quantum number of the Hagedorn state they are building up, being large for $B = S = Q = 0$ and rather small for $B = Q = 1, S = 0$. Another remarkable feature is that for both radii the total decay width tends to a constant value depending only on R for large masses. Having the numerous branching ratios Eq. (6) at hand, one is able to calculate hadronic multiplicities stemming from Hagedorn state decays. Here one starts with some initial heavy Hagedorn state, which decays subsequently down until hadrons are left only as shown in Fig. 3. Among those also non stable resonances might appear, which further undergo a hadronic feed down leaving one with light and stable hadrons with respect to the strong force like pions, kaons, etc. . All hadronic properties used here were taken from the transport model UrQMD [22]. Calculated multiplicities and their ratios for some uncharged ($B = S = Q = 0$) initial Hagedorn state are shown in Fig. 4 (upper part). One observes a linear dependence of all multiplicities on the initial Hagedorn state mass where the magnitude depends on the available phase space for each hadron. Thus in a decay of a charge neutral

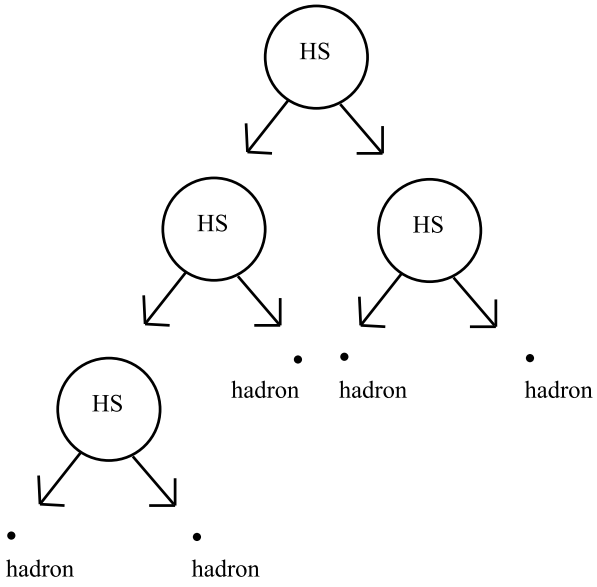

Figure 3. One possible decay chain of an initial heavy HS

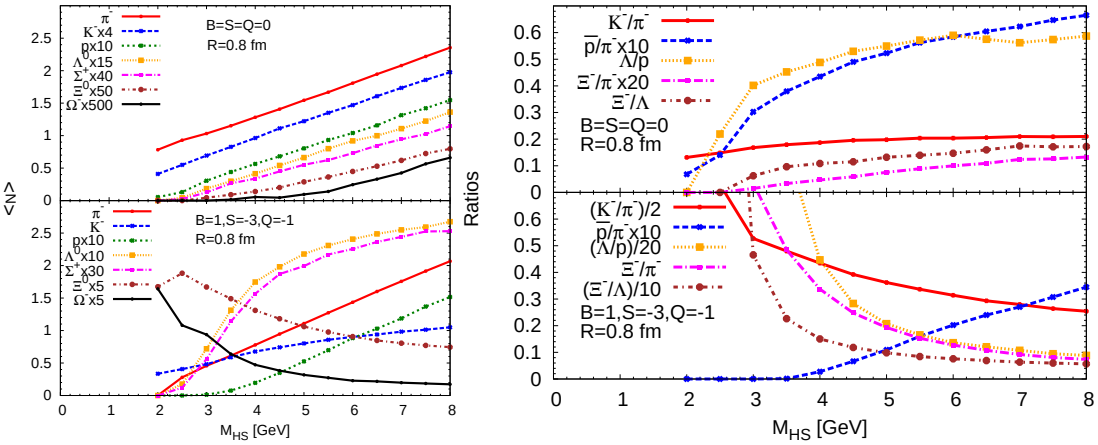

Figure 4. Hadronic multiplicities after a cascade decay of initial Hagedorn state with radius $R = 0.8\,\mathrm{fm}$ and $B = S = Q = 0$ (upper left) and $B = 1, S = -3, Q = -1$ (lower left). Corresponding multiplicity ratios are shown for $B = S = Q = 0$ (upper right) and $B = 1, S = -3, Q = -1$ (lower right). In both cases 'hadronic' feeddown is taken into account.

Hagedorn state π^- clearly expectedly dominate which have to be produced in pairs mostly with π^+ since exact charge conservation is enforced. Kaons, especially K^-, are even stronger suppressed not only of their larger mass but also due to the fact that they have to conserve both electric charge and strangeness. For the baryons presented the same argumentation holds since both have to conserve baryon number B and additionally electric charge Q for proton and strangeness S for Λ. For the multistrange hyperons Ξ^0 and Ω^- the production suppression is even stronger. This has to be contrasted with the results for a baryonic, multi-strange and electrically charged $(B = 1, S = -3, Q = -1)$ Ω^--like Hagedorn state also shown in Fig. 4. Now the choice of Hagedorn state's initial quantum numbers is reflected in the preference of baryon production although they are much heavier than the presented mesons. Especially the abundance of hyperons $\left(\Omega^-, \Xi^0\right)$ compared to the case discussed before is striking since the easiest way to

conserve the initial quantum numbers is the production of one $\Omega^-\pi^0$- or one $\Xi^0 K^-$ pair where on the other hand the phase space for all other hadrons with different quantum numbers is suppressed now. Hence exact conservation of quantum numbers always causes a competition between hadron's phase space and its quantum numbers. On the right part of Fig. 4 the corresponding multiplicity ratios for $R = 0.8\,\mathrm{fm}$ and same quantum number combinations are shown. A comparison of theoretical ratios with experimental results is also provided. Numerical values for the multiplicity ratios for Hagedorn state masses of 4 GeV and 8 GeV are listed in Tab. 1 and, for illustration, compared to experimental results for p-p- and Pb-Pb collisions at midrapidity, both measured by ALICE at LHC. The theoretical multiplicity ratios lie seemingly

	p-p	Pb-Pb	4 GeV	8 GeV
K^-/π^-	0.123(14)	0.149(16)	0.187	0.210
$\overline{p}/\pi^-$	0.053(6)	0.045(5)	0.043	0.066
Λ/π^-	0.032(4)	0.036(5)	0.021	0.038
$\Lambda/\overline{p}$	0.608(88)	0.78(12)	0.494	0.579
Ξ^-/π^-	0.003(1)	0.0050(6)	0.0023	0.0066
$\Omega^-/\pi^- \cdot 10^{-3}$	—	0.87(17)	0.086	0.560

Table 1. Comparison of particle multiplicity ratios from theory vs. p-p at $\sqrt{s_{NN}} = 0.9\,\mathrm{TeV}$ [28] and Pb-Pb at $\sqrt{s_{NN}} = 2.76\,\mathrm{TeV}$ [29, 30, 31], both from ALICE at LHC. Calculated values are listed for Hagedorn state masses of 4 GeV and 8 GeV. Numbers in brackets denote the error in the last digits of the multiplicity ratios.

close to the measured by ALICE, except for the very rare multi-strange baryon Ω^-. However, it has to be made clear, that the decay of HS alone is never assumed to describe the experimental data. The theoretical multiplicity ratios serve as a proof of reliability and reasonability of Hagedorn state's branching ratios defined in Eq. (6). This test is necessary before implementing them into a transport model. Beside multiplicities also the energy distribution of the decay products was examined. They are shown in Fig. 5 for an uncharged ($B = S = Q = 0$) Hagedorn state with initial mass $M_{HS} = 4\,\mathrm{GeV}$ and also $M_{HS} = 8\,\mathrm{GeV}$. The striking observations are that all particle species follow a Boltzmann-like distribution with the same slope independent on the initial Hagedorn state mass. Thus pions, kaons, protons spectra look alike stemming of a system with a temperature being $T_{th} = 0.162\,\mathrm{GeV}$. We remark that the final and freely moving hadrons are freed from the subsequent decays without any reintaractions. The particular finding is that the 'thermal' temperature T_{th} exactly equals the Hagedorn temperature T_H obtained from a fit in the left part of Fig. 1 for the case $R = 0.8\,\mathrm{fm}$. The Hagedorn temperature T_H was nothing but a slope parameter to fit the exponential part of the Hagedorn spectrum, where on the other hand T_{th} is the slope ('temperature') of the finally created hadrons. Starting with a bootstrap formula with no introduction of any notion of temperatures at all resulted in a 'thermalized' decay with a slope being the Hagedorn temperature.

4. Conclusion

A covariantly formulated bootstrap equation is presented which ensures energy and quantum number conservation. The solution of this bootstrap equation provides the Hagedorn spectra describing the 'hadronic' part adequately and being exponential for large masses. Given the Hagedorn spectra the total decay width formula for HS was presented which was obtained on the principle of detailed balance between their creation and their decay. The main characteristics of HS' total decay width are their large peaks for masses in the 'hadronic' range and roughly

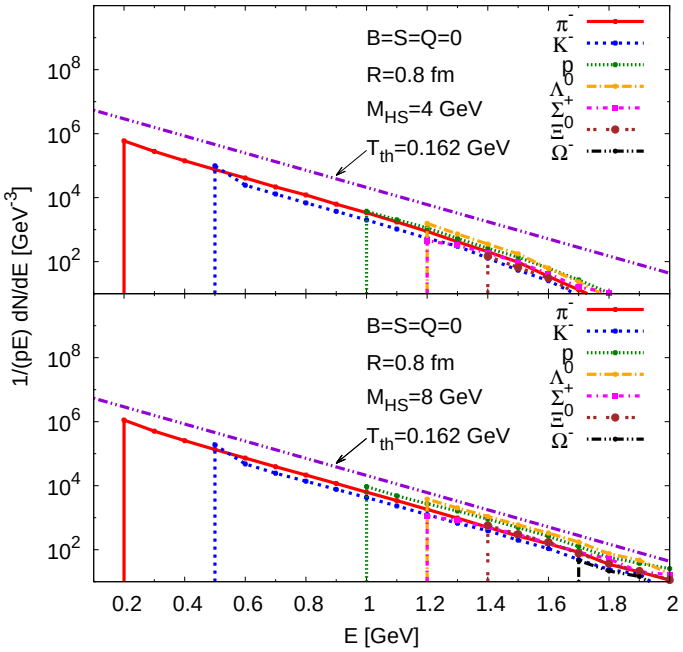

Figure 5. Energy spectra of hadrons stemming from cascade decay of charge neutral Hagedorn state with radius $R = 0.8\,\mathrm{fm}$ and initial mass $M_{HS} = 4\,\mathrm{GeV}$ and $M_{HS} = 8\,\mathrm{GeV}$.

constant values for masses beyond that range. With partial and total decay width we were able to define HS' branching ratios needed for decay simulations. As a specific case we considered decay chains of one single initial Hagedorn state cascading down by various two (intermediate) particle decay channels until stable hadrons were left only. The multiplicity ratios of those stable hadrons where compared to Pb-Pb ALICE data at LHC to check the reasonability and reliability of HS' theoretical branching ratios. Also the energy distribution of those hadrons were examined for two initial HS' masses. The striking findings were that all hadrons stemming from such a decay chain, without any reinteractions, are first all thermal and second exhibit the same temperature. The particular feature of this 'thermal' temperature is that it equals the Hagedorn temperature gained from a fit of Hagedorn spectrum's exponential part. Summarizing, such a finding gives fresh insight into the microscopic and thermal-like hadronization in ultrarelativistic e^+-e^-- (see eg. [32]), hadron-hadron-, and also especially in heavy ion collisions: An implementation of the presented Hagedorn state decays in addition to their production mechanisms into the transport approach UrQMD offers a new venue for allowing strongly interacting hadronic multiparticle collisions in a consistent scheme being important in the vicinity of the deconfinement transition by creating and decaying more exotic HS. Understanding faster thermalization and chemical equilibration, but also microscopic transport properties can be thoroughly investigated in future [21].

5. Acknowledgements

The authors acknowledges discussions with K. Bugaev. This work was supported by the Bundesministerium für Bildung und Forschung (BMBF), the HGS-HIRe and the Helmholtz International Center for FAIR within the framework of the LOEWE program launched by the State of Hesse. Numerical computations have been performed at the Center for Scientific Computing (CSC).

References

[1] Hagedorn R 1965 *Nuovo Cim. Suppl.* **3** 147–186
[2] Greiner C and Leupold S 2001 *J. Phys. G* **27** L95–L102
[3] Greiner C, Koch-Steinheimer P, Liu F M, Shovkovy I A and Stoecker H 2005 *J. Phys. G* **31** S725–S732
[4] Noronha-Hostler J, Greiner C and Shovkovy I A 2008 *Phys. Rev. Lett.* **100** 252301
[5] Noronha-Hostler J, Greiner C and Shovkovy I 2010 *J. Phys. G* **37** 094017
[6] Noronha-Hostler J, Beitel M, Greiner C and Shovkovy I 2010 *Phys. Rev. C* **81** 054909
[7] Moretto L, Bugaev K, Elliott J and Phair L 2006 *Europhys. Lett.* **76** 402–408
[8] Zakout I, Greiner C and Schaffner-Bielich J 2007 *Nucl. Phys. A* **781** 150–200
[9] Zakout I and Greiner C 2008 *Phys. Rev. C* **78** 034916
[10] Ferroni L and Koch V 2009 *Phys. Rev. C* **79** 034905
[11] Bugaev K, Petrov V and Zinovjev G 2009 *Phys. Rev. C* **79** 054913
[12] Ivanytskyi A, Bugaev K, Sorin A and Zinovjev G 2012 *Phys. Rev. E* **86** 061107
[13] Noronha-Hostler J, Noronha J and Greiner C 2009 *Phys. Rev. Lett.* **103** 172302
[14] Majumder A and Muller B 2010 *Phys. Rev. Lett.* **105** 252002
[15] Karsch F, Redlich K and Tawfik A 2003 *Eur.Phys.J.* **C29** 549–556
[16] Noronha-Hostler J, Noronha J and Greiner C 2012 *Phys. Rev. C* **86** 024913
[17] Jakovac A 2013 *Phys. Rev. D* **88** 065012
[18] Gorenstein M, Hauer M and Moroz O 2008 *Phys. Rev. C* **77** 024911
[19] Itakura K, Morimatsu O and Otomo H 2008 *J. Phys. G* **35** 104149
[20] Noronha-Hostler J, Ahmad H, Noronha J and Greiner C 2010 *Phys. Rev. C* **82** 024913
[21] Beitel M, Gallmeister K and Greiner C 2014 in preparation
[22] Bass S, Belkacem M, Bleicher M, Brandstetter M, Bravina L *et al.* 1998 *Prog. Part. Nucl. Phys.* **41** 255–369
[23] Frautschi S C 1971 *Phys. Rev. D* **3** 2821–2834
[24] Hamer C and Frautschi S C 1971 *Phys. Rev. D* **4** 2125–2137
[25] Beringer J *et al.* (Particle Data Group) 2012 *Phys. Rev. D* **86**(1) 010001
[26] Yellin J 1973 *Nucl. Phys. B* **52** 583–594
[27] Hagedorn R and Montvay I 1973 *Nucl. Phys. B* **59** 45–86
[28] Aamodt K *et al.* (ALICE Collaboration) 2011 *Eur. Phys. J. C* **71** 1594
[29] Abelev B *et al.* (ALICE Collaboration) 2013 *Phys. Rev. C* **88** 044910
[30] Abelev B B *et al.* (ALICE Collaboration) 2013 *Phys. Rev. Lett.* **111** 222301
[31] Abelev B B *et al.* (ALICE Collaboration) 2014 *Phys. Lett. B* **728** 216–227
[32] Becattini F 1996 *Z. Phys. C* **69** 485–492

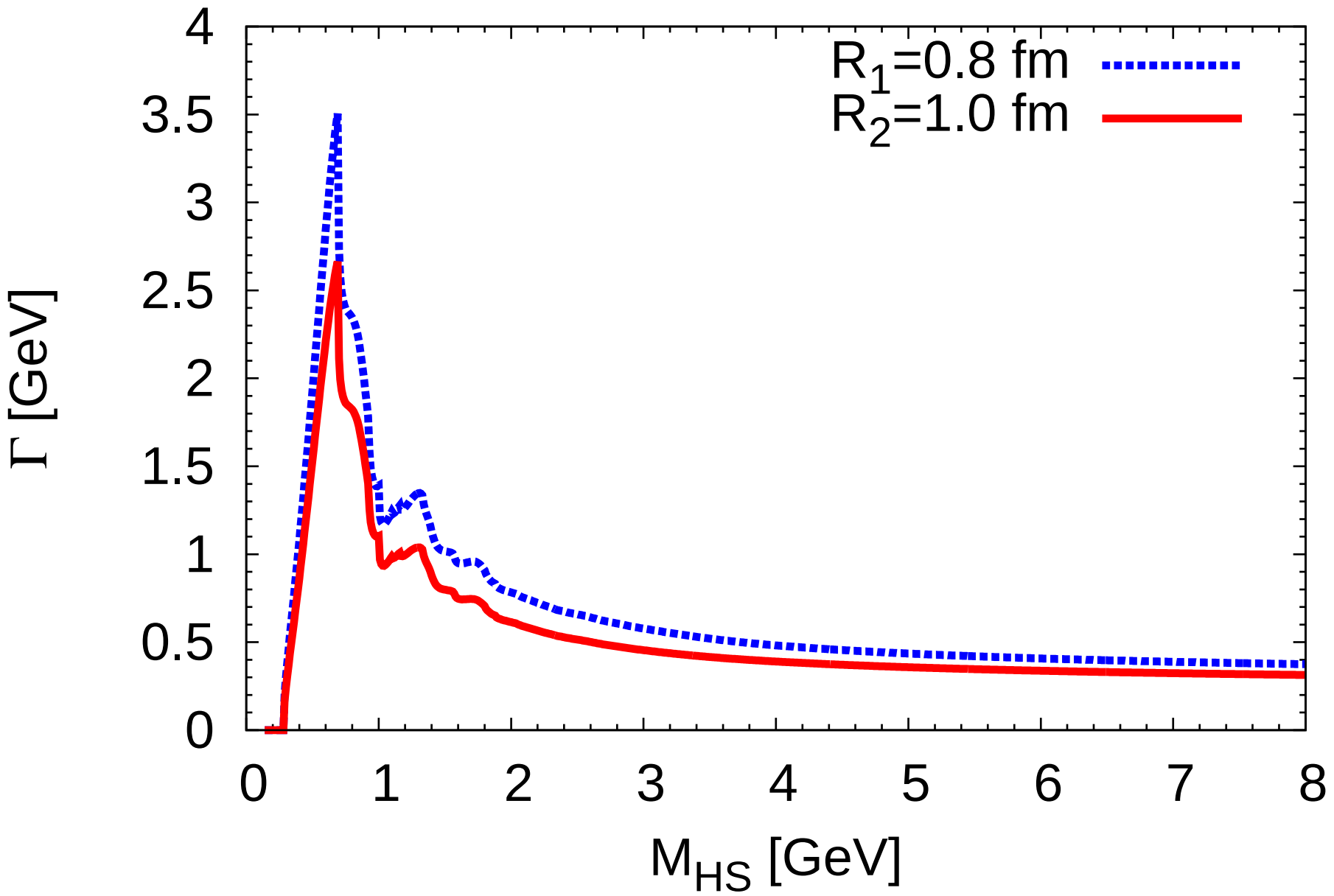
R1=0.8 fm
R2=1.0 fm
Γ [GeV]
M_HS [GeV]
0
0.5
1
1.5
2
2.5
3
3.5
4
0
1
2
3
4
5
6
7
8

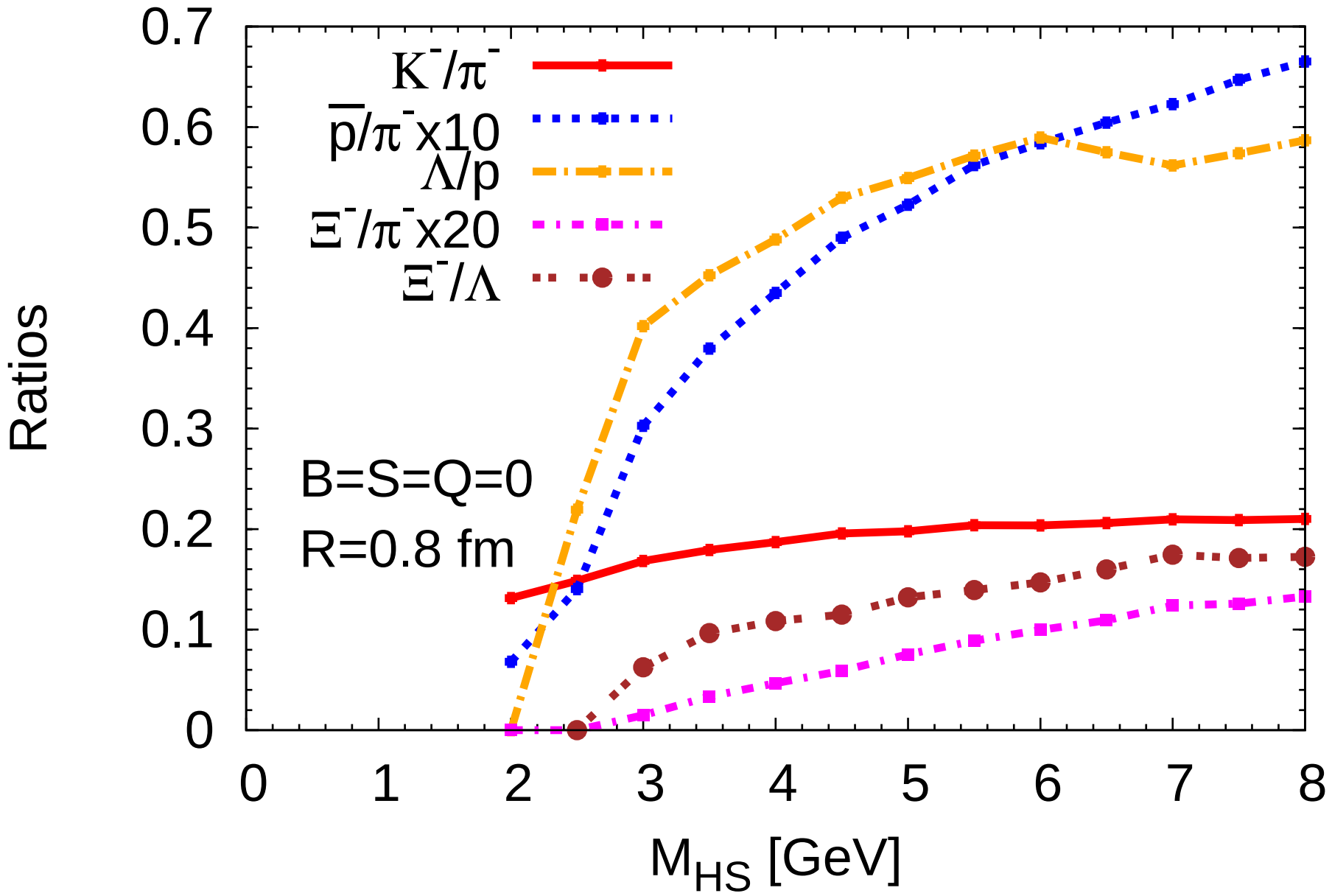
0.7
0.6
0.5
0.4
0.3
0.2
0.1
0
Ratios
0
1
2
3
4
5
6
7
8
M_{HS} [GeV]
K^-/π^-
$\bar{p}/\pi^-$x10
Λ/p
Ξ^-/π^-x20
Ξ^-/Λ
B=S=Q=0
R=0.8 fm